JAERI-M
88-037

INFLUENCE OF BACKGROUND NEUTRALS ON CHARGE EXCHANGE NEUTRAL SPECTRA IN OHMICALLY HEATED JT-60 PLASMAS

February 1988

Kenji TOBITA, Yoshinori KUSAMA, Masahiro NEMOTO
Hiroshi TAKEUCHI, Masafumi AZUMI and JT-60 Team

日本原子力研究所
Japan Atomic Energy Research Institute

JAERI-M レポートは，日本原子力研究所が不定期に公刊している研究報告書です。
入手の問合わせは，日本原子力研究所技術情報部情報資料課（〒319—11 茨城県那珂郡東海村）あて，お申しこしください。なお，このほかに財団法人原子力弘済会資料センター（〒319-11 茨城県那珂郡東海村日本原子力研究所内）で複写による実費頒布をおこなっております。

JAERI-M reports are issued irregularly.
Inquiries about availability of the reports should be addressed to Information Division, Department of Technical Information, Japan Atomic Energy Research Institute, Tokai-mura, Naka-gun, Ibaraki-ken 319-11, Japan.

編集兼発行　日本原子力研究所
印　　刷　山田軽印刷所

JAERI-M 88-037

Influence of Background Neutrals on Charge Exchange Neutral Spectra in Ohmically Heated JT-60 Plasmas

Kenji TOBITA, Yoshinori KUSAMA, Masahiro NEMOTO
Hiroshi TAKEUCHI, Masafumi AZUMI and JT-60 Team※

Department of Large Tokamak Research
Naka Fusion Research Establishment
Japan Atomic Energy Research Institute
Naka-machi, Naka-gun, Ibaraki-ken

(Received January 29, 1988)

Neutrals emitted from ohmically heated JT-60 plasmas were measured by two neutral particle analysers with different sight-lines. Measured charge exchange spectra presented clear distortion arising from poloidal asymmetry of neutral sources. Ion temperature from charge exchange measurements was 10 - 30% less than the central temperature at $\bar{n}_e$ = (0.5-4.0) × 10^{19} m^{-3}. From the magnitude of the spectra, we determined the neutral density in the core region. At $\bar{n}_e \lesssim 2.5 \times 10^{19}$ m^{-3}, the obtained neutral density n_0 decreased as $\bar{n}_e$ increased, and agreed with the neutral density expected by electron-ion recombination alone at $\bar{n}_e$ = (2.5-4.0) × 10^{19} m^{-3}. The result indicates that the neutral density in the core region is determined by penetration of cold neutrals and their generations at $\bar{n}_e \lesssim 2.5 \times 10^{19}$ m^{-3}, and also shows that at $\bar{n}_e \gtrsim 2.5 \times 10^{19}$ m^{-3} the neutrals are mainly generated by recombination of protons and electrons.

Keywords: JT-60, Charge Exchange, Neutral Density, Ion Temperature, Recombination

※

T.ABE, H.AIKAWA, N.AKAOKA, H.AKASAKA, M.AKIBA, N.AKINO, T.AKIYAMA, T.ANDO
K.ANNOH, T.AOYAGI, T.ARAI, K.ARAKAWA, M.ARAKI, K.ARIMOTO, M.AZUMI, S.CHIBA
M.DAIRAKU, N.EBISAWA, T.FUJII, T.FUKUDA, A.FUNAHASHI, H.FURUKAWA
K.HAMAMATSU, M.HANADA, M.HARA, K.HARAGUCHI, H.HIRATSUKA, T.HIRAYAMA, S.HIROKI
K.HIRUTA, M.HONDA, M.HONDA, H.HORIIKE, R.HOSODA, N.HOSOGANE, Y.IIDA, T.IIJIMA
K.IKEDA, Y.IKEDA, T.IMAI, T.INOUE, N.ISAJI, M.ISAKA, S.ISHIDA, K.ITAMI
N.ITIGE, T.ITO, Y.ITO, T.KAKIZAKI, A.KAMINAGA, T.KATO, M.KAWAI, M.KAWABE
Y.KAWAMATA, K.KAWASAKI, K.KIKUCHI, M.KIKUCHI, H.KIMURA, T.KIMURA, H.KISHIMOTO
K.KITAHARA, S.KITAMURA, A.KITSUNEZAKI, K.KIYONO, N.KOBAYASHI, K.KODAMA
S.KOIDE, Y.KOIDE, T.KOIKE, M.KOMATA, I.KONDO, S.KONOSHIMA, H.KUBO, S.KUNIEDA
K.KURIHARA, M.KURIYAMA, T.KURODA, M.KUSAKA, Y.KUSAMA, Y.MABUTI, S.MAEHARA
K.MAENO, T.MATOBA, S.MATSUDA, M.MATSUKAWA, T.MATSUKAWA, M.MATSUOKA, Y.MIURA
N.MIYA, K.MIYACHI, Y.MIYO, K.MIZUHASHI, M.MIZUNO, M.MORI, S.MORIYAMA, R.MURAI
Y.MURAKAMI, M.MUTO, M.NAGAMI, A.NAGASHIMA, K.NAGASHIMA, T.NAGASHIMA, S.NAGAYA
O.NAITO, H.NAKAMURA, Y.NAKAMURA, M.NEMOTO, Y.NEYATANI, H.NINOMIYA, N.NISHINO
T.NISHITANI, H.NOMATA, K.OBARA, H.OBINATA*5, Y.OGAWA, N.OGIWARA, T.OHGA
Y.OHARA, K.OHASA, H.OOHARA, T.OHSHIMA, M.OHKUBO, S.OHSAWA, K.OHTA, M.OHTA
M.OHTAKA, Y.OHUCHI, A.OIKAWA, H.OKUMURA, Y.OKUMURA, K.OMORI, S.OMORI, Y.OMORI
T.OZEKI, M.SAEGUSA, N.SAITOH, K.SAKAMOTO, A.SAKASAI, S.SAKATA, T.SASAJIMA
K.SATOU, M.SATOU, M.SATOU, A.SAKURAI, M.SAWAHATA, T.SEBATA*4, M.SEIMIYA
M.SEKI, S.SEKI, K.SHIBANUMA, R.SHIMADA, T.SHIMADA*4, K.SHIMIZU, M.SHIMIZU
Y.SHIMOMURA, S.SHINOZAKI, H.SHIRAI, H.SHIRAKATA, M.SHITOMI, K.SUGANUMA
T.SUGIE, T.SUGIYAMA, H.SUNAOSHI, K.SUZUKI, M.SUZUKI, M.SUZUKI, N.SUZUKI
N.SUZUKI, S.SUZUKI, Y.SUZUKI, M.TAKAHASHI, S.TAKAHASHI, T.TAKAHASHI
M.TAKASAKI, H.TAKATSU, H.TAKEUCHI, A.TAKESHITA, T.TAKIZUKA, S.TAMURA
S.TANAKA, T.TANAKA, K.TANI, M.TERAKADO, T.TERAKADO, K.TOBITA, T.TOKUTAKE
T.TOTSUKA, N.TOYOSHIMA, F.TSUDA, T.TSUGITA, S.TSUJI, Y.TSUKAHARA, M.TSUNEOKA
K.UEHARA, M.UMEHARA, Y.URAMOTO, H.USAMI, K.USHIGUSA, K.USUI, J.YAGYU
M.YAMAGIWA, T.YAMAGUCHI, M.YAMAMOTO, T.YAMAMOTO, O.YAMASHITA, Y.YAMASHITA
T.YAMAZAKI, T.YASUKAWA, K.YOKOKURA, H.YOKOMIZO, K.YOKOYAMA, K.YOSHIKAWA
M.YOSHIKAWA, H.YOSHIDA, Y.YOSHINARI, R.YOSHINO, Y.YOSHIOKA*4, I.YONEKAWA
T.YONEDA, K.WATANABE, R.GOLDSTON*1, F.SÖLDNER*2, Y.TAKASE*3, K.WONG*1

*1 Princeton Plasma Physics Laboratory, USA
*2 Max-Planck-Institut für Plasmaphysik, West Germany
*3 Massachusetts Institute of Technology, USA
*4 Contract Researcher
*5 Kyushu University

JAERI－M 88－037

JT－60ジュール加熱プラズマにおけるバックグラウンド中性粒子の荷電交換中性粒子スペクトルに与える影響

日本原子力研究所那珂研究所臨界プラズマ研究部
飛田　健次・草間　義紀・根本　正博・竹内　　浩
安積　正史・JT－60チーム※

（1988年1月29日受理）

JT－60のジュール加熱プラズマから放出される中性粒子のエネルギースペクトルを2台の中性粒子分析器を用いて測定した。測定された中性粒子スペクトルは，粒子リサイクリングによる中性粒子源の分布がポロイダル非対称であることを示した。スペクトルの傾きから得られたイオン温度は，$\overline{n_e}=(0.5-4.0)\times10^{19}\,m^{-3}$ の領域で，中心イオン温度より10－30％低かった。また，スペクトルの強度から，中心付近の中性粒子密度が求められた。その密度は，$\overline{n_e}<2.5\times10^{19}\,m^{-3}$ の領域で $\overline{n_e}$ の増加と伴に減少し，$\overline{n_e}\approx(2.5-4.0)\times10^{19}\,m^{-3}$ では電子－イオン再結合から期待される密度に一致した。この結果は，$\overline{n_e}\gtrsim2.5\times10^{19}\,m^{-3}$ のとき，プラズマ中心付近の中性粒子は主に電子－イオン再結合で生成されることを示す。

※那珂研究所：〒311－01 茨城県那珂郡那珂町大字向山801－1

※ 相川 裕史・青柳 哲雄・赤岡 伸雄・赤坂 博美・秋野 昇・秋場 真人・秋山 隆
安積 正史・阿部 哲也・新井 貴・荒川喜代次・荒木 政則・有本 公子・安東 俊郎
安納 勝人・飯島 勉・飯田 幸生・池田 幸治・池田 佳隆・井坂 正義・伊佐治信明
石田 真一・伊丹 潔・市毛 尚志・伊藤 孝雄・伊藤 康治・井上多加志・今井 剛
上原 和也・宇佐美広次・牛草 健吉・薄井 勝富・梅原 昌敏・浦本 保幸・海老沢 昇
及川 晃・大麻 和美・大内 豊・大賀 徳道・大久保 実・大沢 悟・大島 貴幸
太田 和也・太田 充・大高 光夫・大原比呂志・大森憲一郎・大森 俊造・大森 栄和
小川 芳郎・荻原 徳男・奥村 裕司・奥村 義和・小関 隆久・小原建治郎・小原 祥裕
大日方裕彦[*5]・柿崎 禎之・加藤 次男・神永 敦嗣・河合視己人・川崎 幸三・川辺 勝
川俣 陽一・菊池 勝美・菊池 満・岸本 浩・北原 勝美・北村 繁・狐崎 晶雄
木村 豊秋・木村 晴行・清野 公広・日下 誠・草間 義紀・国枝 俊介・久保 博孝
栗原 研一・栗山 正明・黒田 猛・小池 常之・小出 真路・小出 芳彦・児玉 幸三
木島 滋・小林 則幸・小又 将夫・近藤 育朗・斉藤 直之・三枝 幹雄・逆井 章
坂田 信也・坂本 慶司・桜井 明・笹島 唯之・佐藤 一也・佐藤 正泰・佐藤 稔
沢畠 正之・鄙 守正・篠崎 信一・柴沼 清・島田 徹[*4]・嶋田 隆一・清水 勝宏
清水 正亜・下村 安夫・白井 浩・白形 弘文・菅沼 和明・杉江 達夫・杉山 隆
鈴木 貞明・鈴木 國弘・鈴木 紀男・鈴木 紀男・鈴木 正信[*4]・鈴木 道雄・鈴木 康夫
砂押 秀則・清宮 宗孝・関 正美・関 省吾・瀬端 毅[*4]・高崎 學・高津 英幸
高橋 春次・高橋虎之助・高橋 実・滝塚 知典・竹内 浩・竹下 明・田中 茂
田中竹次郎・谷 啓二・田村 早苗・大楽 正幸・千葉 真一・塚原 美光・次田 友宜
辻 俊二・津田 文男・恒岡まさき・寺門 恒久・寺門 正之・徳竹 利国・戸塚 俊之
飛田 健次・豊島 昇・内藤 磨・中村 博雄・中村 幸治・長島 章・永島 圭介
永島 孝・永谷 進・永見 正幸・西谷 健夫・西野 信博[*4]・二宮 博正・根本 正博
閨谷 譲・野亦 英幸・花田磨砂也・濱松 清隆・原 誠・原口 和三・平塚 一
平山 俊雄・蛭田 和治・廣木 成治・福田 武司・藤井 常幸・船橋 昭昌・古川 弘
細金 延幸・細田隆二郎・堀池 寛・本田 正男・本多 光輝・前野 勝樹・前原 直
松岡 守・松川 達哉・松川 誠・松田慎三郎・的場 徹・間淵 幸雄・三浦 良和
水野 誠・水橋 清・宮 直之・宮地 謙吾・三代 康彦・武藤 貢・村井 隆一
村上 義夫・森 雅博・森山 伸一・柳生 純一・安川 享・山極 満・山崎 武
山下 修・山下 幸彦・山口 健・山本 巧・山本 正弘・横倉 賢治・横溝 英明
横山 堅二・吉岡 祐二[*4]・吉川 和伸・吉川 允二・吉田 英俊・吉成 洋治・芳野 隆治
米川 出・米田 毅・渡邊 和弘・Y. Takase[*3]・K. Wong[*1]・R. Goldston[*1]・F. Söldner[*2]

* 1 Princeton Plasma Physice Laboratory, U.S.A.
* 2 Max-Planck-Institute für Plasmaphysik, West Germany
* 3 Massachusetts Institute of Technology, U.S.A.
* 4 外来研究員
* 5 九州大学

Contents

目　　次

1. Introduction

Laboratory plasmas contain traces of neutral atoms owing to transport of incoming cold neutrals and recombination of protons and electrons($H^{+}+e\text{--->}H^{0}$). Plasma ions undergo charge exchange reaction with these neutrals and then a part of them escapes from the plasma. The energy analysis of the neutral efflux has been used to measure the ion temperature and the energy distribution of the plasma ions in many fusion devices.

In large tokamaks like JT-60, a high line-density plasma satisfying $\sigma_{cx}\bar{n}a>>1$ (where σ_{cx} the cross section for resonance charge exchange of hydrogen ions and atoms, and $\bar{n}$ and a are mean plasma density and a minor radius, respectively) is readily produced with increasing $\bar{n}$. For such a dense plasma, the probability of neutrals penetrating deep into the plasma and that of charge-exchanged neutrals escaping to the outside from the central region of the plasma are significantly reduced. As a result, the charge exchange spectra reflect the ion energy distributuion in the periphery rather than in the center. Moreover, the shortness of the mean free path of neutrals implies that localization of neutral sources outside the plasma causes poloidal and/or toroidal asymmetry of neutral density profile in the plasma. The asymmetry probably affects spectra of neutrals emitted from the plasma. It is, therefore, of great importance to investigate the influence of background neutrals on the charge exchange neutral spectra when we infer the local energy distribution from the measured spectra.

Up to now, charge exchange diagnostics of plasmas with high line-density have been reported on Alcator. Gaudreau et al.[1] investigated fast atom fluxes in the high density plasma in the Alcator

tokamak. Assuming that energetic atoms with the energy of 4 - 6 keV are only emitted from the central plasma, they estimated the neutral density required for the production of the measured flux was equal to 10^{13}-$10^{14}m^{-3}$ at $\bar{n}_e$=$5\times10^{20}m^{-3}$. Dnestrovskij et al.[2] compared the calculated neutral flux and spectra with the measured values for the dense Alcator plasma, and concluded that on the Alcator device the main mechanism producing neutrals in the central plasma at $n>4\times10^{20}m^{-3}$ was recombination of protons and electrons.

In large tokamaks, the recombination process may be dominant neutral-production mechanism at much lower plasma density. In order to investigate, in the JT-60 plasmas, the density region where the central neutrals are mainly produced by the recombination, we here estimated the neutral density from the magnitude of fast neutral.

This paper is organized in the following manner. Section 2 presents the description on the experimental parameters and the neutral particle analysers. Section 3 describes the influence of asymmetry of neutral sources on the spectra in ohmically heated JT-60 plasmas. Characteristics of the charge exchange spectra on JT-60 are presented in this section. In section 4, ion temperature from charge exchange is described according to experimental data and numerical analysis. Section 5 gives the result of the central neutral density measurement.

2. Description of Charge Exchange Diagnostics

Our studies were performed in the ohmically heated plasmas of the JT-60 tokamak.[3] The JT-60 machine is typically discharged for 10s with a major radius $R \cong 3m$, minor radius $a \cong 0.95m$ in limiter and $a \cong 0.86m$ in the divertor configuration, toroidal field $B_T = 3.0\text{-}4.7T$, plasma current $I_p = 0.7\text{-}3.2MA$, and duration of current flat-top up to 7 s. The working gas was hydrogen which was feeded either from the divertor chamber or from the main chamber.

Charge-exchanged neutral efflux from the plasma was measured by two neutral particle analysers (the divertor-side NPA and the vertical NPA) which are installed in JT-60 along different sight-lines. The divertor-side NPA is an electrostatic energy analyser[4] with a charge-stripping cell, 45° deflection plates, 48ch ion detectors (micro-channel plate detectors, MCP), a pulse counting system and a data acquisition system. The vertical NPA is an E//B type mass-separated analyser[5] which has electric and magnetic fields in same direction. The observation solid angles, $\Delta\Omega$, are 1.8×10^{-7} for the divertor-side and 9.0×10^{-8} for the vertical NPA. Figure 1 shows the poloidal cross section of JT-60 and the sight-lines of these NPAs. These NPAs view the plasma center, perpendicularly to the magnetic field lines. In this geometry, the NPAs observe trapped ions with $v_{//}/v \cong 0$. The vertical NPA is placed on the ion drift side. Drift motion of fast ions enhances the population of the high-energy ions in charge exchange spectra observed along this direction owing to the vertical shift of high-energy ions.[6] In our case, however, there is only an insignificant shift of the spatial distribution of high-energy ions, compared with the distribution of low-energy ions. The shift due to grad-B drift,

Δr, is estimated by the equation[1], $\Delta r \cong v_{dr} \bar{\delta} \nu_{ii}^{-1}$. Here v_{dr} is the toroidal drift velocity, $\bar{\delta}$ the ripple of the magnetic field ($\Delta B/B$) and ν_{ii} the ion-ion collision frequency. Substituting our experimental parameters, $\bar{\delta}=10^{-4}$, $\bar{n}_i=1\times10^{19}m^{-3}$, $B_T=4.0T$, $T_i=2.5keV$ and $E=20keV$, we have $\Delta r\cong3\times10^{-3}m$. This value is much smaller than the minor radius a ($\cong$ 0.86m). Therefore the drift motion of trapped ions causes little effect on the high-enery ion distribution.

3. Characteristics of Charge Exchange Spectra

Hα emissivity measurements have indicated that neutral source is strongly localized on the divertor side in the diverted JT-60 plasma.[7] Such poloidal asymmetry of neutral sources may cause the distortion of the charge exchange spectra. In this section, we describe the characteristics of the spectra, in particular, the influence of the asymmetry on the spectra.

Here we explain the observed charge exchange spectra in a limiter discharge changing to the divertor configuration at 4.3 sec. Figure 2 shows the most outer magnetic surface in the shot. These magnetic surfaces were obtained by a poloidal magnetic fitting code with the current-filaments approximation of magnetic probe signals.[8] In the limiter configuration the plasma contacts with inner limiters. In the divertor configuration the plasma column shifts outside and does not touch any limiters. Time evolution of $\bar{n}_eL$, input gas speed (Q) and Hα emissivities is shown in Fig.3 (a). Figure 3 (b) shows the sight-lines of photo-diodes for Hα measurements. In this shot, the limiter configuration shown in Fig.2 (a) is formated at 1.0-4.0s, and the plasma

Δr, is estimated by the equation[1], $\Delta r \simeq v_{dr} \bar{\delta} \nu_{ii}^{-1}$. Here v_{dr} is the toroidal drift velocity, $\bar{\delta}$ the ripple of the magnetic field ($\Delta B/B$) and ν_{ii} the ion-ion collision frequency. Substituting our experimental parameters, $\bar{\delta}=10^{-4}$, $\bar{n}_i=1\times10^{19}m^{-3}$, $B_T=4.0T$, $T_i=2.5keV$ and $E=20keV$, we have $\Delta r \simeq 3\times10^{-3}m$. This value is much smaller than the minor radius a ($\simeq$ 0.86m). Therefore the drift motion of trapped ions causes little effect on the high-enery ion distribution.

3. Characteristics of Charge Exchange Spectra

Hα emissivity measurements have indicated that neutral source is strongly localized on the divertor side in the diverted JT-60 plasma.[7] Such poloidal asymmetry of neutral sources may cause the distortion of the charge exchange spectra. In this section, we describe the characteristics of the spectra, in particular, the influence of the asymmetry on the spectra.

Here we explain the observed charge exchange spectra in a limiter discharge changing to the divertor configuration at 4.3 sec. Figure 2 shows the most outer magnetic surface in the shot. These magnetic surfaces were obtained by a poloidal magnetic fitting code with the current-filaments approximation of magnetic probe signals.[8] In the limiter configuration the plasma contacts with inner limiters. In the divertor configuration the plasma column shifts outside and does not touch any limiters. Time evolution of $\bar{n}_e L$, input gas speed (Q) and Hα emissivities is shown in Fig.3 (a). Figure 3 (b) shows the sight-lines of photo-diodes for Hα measurements. In this shot, the limiter configuration shown in Fig.2 (a) is formated at 1.0-4.0s, and the plasma

is diverted at 4.3-7.0s. Higher Hα emissivity in the main chamber is observed in $H\alpha^{main}$-1 for the limiter configuration, and in $H\alpha^{main}$-4 for the divertor configuration. This indicates that neutral sources are located near the limiters touching with the plasma in the limiter configuration, and near the divertor throat in the divertor configuration. Figure 4 (a) shows time evolution of charge exchange flux measured by the vertical NPA. Each solid line represents the outflux of neutrals having the energy of 3*keV*, 6*keV* and 10*keV*. Rapid evolution of the fluxes at t=4.0-4.5s is due to the shift of the limiters interacting with the plasma. The fluxes in the limiter configuration are higher than those in the divertor configuration because there is a strong neutral source (recycling neutrals) near the sight-line of the NPA, as shown by arrows in Fig.2 (a). Figure 4 (b) shows time evolution of charge exchange fluxes measured by the divertor-side NPA. As shown in the figure, the charge exchange fluxes are considerably higher in the divertor configuration. This enhancement of the fluxes is probably caused by refuelling neutrals: a part of neutrals compressed into the divertor chamber flows backward and then recycles into the divertor-side main plasma. The expected particle flows are illustrated by arrows in Fig.2 (b).

Charge exchange spectra observed by both NPAs in the limiter and divertor configurations are shown in Fig.5. In these spectra the observation volumes and the observation solid angles of the NPAs are corrected to compare the magnitude of the charge exchange fluxes viewed along both directions. In the limiter configuration, the enhancement of the neutral fluxes is observed especially in the low energy region of the vertical charge exchange spectrum. In the divertor configuration, the similar enhancement is observed in the divertor-side

spectrum. These results support the poloidal asymmetry of neutral sources. Since the plasma contacts with the toroidal fixed limiter near the sight-line of the vertical NPA in the limiter configuration, the NPA observes the enhancement of low-energy neutral fluxes during the configuration. The divertor-side NPA, on the contrary, observes more charge exchange fluxes in the divertor discharges, because of the refuelling of neutrals from the divertor chamber. In the high energy region of the spectra, however, there is no difference of the magnitude on observation direction in both figures. This is because the high-energy nuetral fluxes reflect the neutral density in the central plasma.

4. Plasma Opacity and Ion Temperature

For low or moderate line electron density, the plasma is transparent for the charge-exchanged neutrals and the ion temperature obtained by charge exchange measurements reflects actual value in the core plasma. However, for the plasmas with high line-density, the temperature from charge exchange measurements underestimates the central ion temperature because the fast neutrals generated in the core hardly traverse the plasmas. In this section, we describes the plasma opacity and the ion temperature from charge exchange.

In order to study the influence of the plasma opacity and the neutral density profile on the ion temperature determination, we adopted a 1-D neutral transport code. With this code, the neutral density profile and charge exchange spectra are calculated using the reasonably assumed plasma density and temperature profiles. Figure 6 shows the ion

spectrum. These results support the poloidal asymmetry of neutral sources. Since the plasma contacts with the toroidal fixed limiter near the sight-line of the vertical NPA in the limiter configuration, the NPA observes the enhancement of low-energy neutral fluxes during the configuration. The divertor-side NPA, on the contrary, observes more charge exchange fluxes in the divertor discharges, because of the refuelling of neutrals from the divertor chamber. In the high energy region of the spectra, however, there is no difference of the magnitude on observation direction in both figures. This is because the high-energy nuetral fluxes reflect the neutral density in the central plasma.

4. Plasma Opacity and Ion Temperature

For low or moderate line electron density, the plasma is transparent for the charge-exchanged neutrals and the ion temperature obtained by charge exchange measurements reflects actual value in the core plasma. However, for the plasmas with high line-density, the temperature from charge exchange measurements underestimates the central ion temperature because the fast neutrals generated in the core hardly traverse the plasmas. In this section, we describes the plasma opacity and the ion temperature from charge exchange.

In order to study the influence of the plasma opacity and the neutral density profile on the ion temperature determination, we adopted a 1-D neutral transport code. With this code, the neutral density profile and charge exchange spectra are calculated using the reasonably assumed plasma density and temperature profiles. Figure 6 shows the ion

temperature ratio, T_i^{CX}/T_{i0} (here T_i^{CX} and T_{i0} represent the ion temperature from charge exchange and the central ion temperature, respectively) as a function of density peaking factor, β_n. Figure 7 also shows T_i^{CX}/T_{i0} as a function of ion temperature peaking factor, β_{Ti}. In these simulations, T_i^{CX} is obtained by fitting the calculated charge exchange spectrum with a straight line in the energy range of 3 - 8 *keV*. The initial energy of neutrals going into the plasma is assumed to be 5 *eV*. In fact, the result is insensitive to the incident energy in the range of 5*eV* to 50*eV*: the difference in T_i^{CX} is less than 5% in this initial energy range. Both these figures indicate that T_i^{CX}/T_{i0} hardly depends on the plasma density and temperature profiles. Figure 8 shows the numerical result of T_i^{CX}/T_{i0} as a function of $\bar{n}_e$. We here assume the density profile of $(1-(r/a)^2)^{0.3}$, from the experimental results in JT-60. And we also assume $n_i(r)=n_e(r)$, T_{e0}=3*keV* and T_{i0}=2*keV*. As shown in the figure, charge exchange measurements underestimate T_{i0} by 10 to 30 % at $0.5\times10^{19}<\bar{n}_e<4\times10^{19}m^{-3}$.

T_i^{CX} was compared with T_{i0} estimated from Rutherford scattering measurements.[9] These experiments were performed in the diverted hydrogen discharges having toroidal field B_T=3.0-4.5*T*, plasma current I_p=0.7-2.0*MA* and line-avaraged electron density $\bar{n}_e=(0.5-4)\times10^{19}m^{-3}$. T_i^{CX} was determined from the non-distorted spectra of the vertical NPA for the reason described in Sec.3. As shown in Fig.9, T_i^{CX} is 10 - 30 % lower than T_{i0}. This result is consistent with the above numerical analysis.

5. Neutral Density Measurement

Figure 10 shows the charge exchange spectra by the vertical NPA,

temperature ratio, T_i^{CX}/T_{i0} (here T_i^{CX} and T_{i0} represent the ion temperature from charge exchange and the central ion temperature, respectively) as a function of density peaking factor, β_n. Figure 7 also shows T_i^{CX}/T_{i0} as a function of ion temperature peaking factor, β_{Ti}. In these simulations, T_i^{CX} is obtained by fitting the calculated charge exchange spectrum with a straight line in the energy range of 3 - 8 *keV*. The initial energy of neutrals going into the plasma is assumed to be 5 *eV*. In fact, the result is insensitive to the incident energy in the range of 5*eV* to 50*eV*: the difference in T_i^{CX} is less than 5% in this initial energy range. Both these figures indicate that T_i^{CX}/T_{i0} hardly depends on the plasma density and temperature profiles. Figure 8 shows the numerical result of T_i^{CX}/T_{i0} as a function of $\bar{n}_e$. We here assume the density profile of $(1-(r/a)^2)^{0.3}$, from the experimental results in JT-60. And we also assume $n_i(r)=n_e(r)$, T_{e0}=3*keV* and T_{i0}=2*keV*. As shown in the figure, charge exchange measurements underestimate T_{i0} by 10 to 30 % at $0.5\times10^{19}<\bar{n}_e<4\times10^{19}m^{-3}$.

T_i^{CX} was compared with T_{i0} estimated from Rutherford scattering measurements.[9] These experiments were performed in the diverted hydrogen discharges having toroidal field B_T=3.0-4.5*T*, plasma current I_p=0.7-2.0*MA* and line-avaraged electron density $\bar{n}_e=(0.5-4)\times10^{19}m^{-3}$. T_i^{CX} was determined from the non-distorted spectra of the vertical NPA for the reason described in Sec.3. As shown in Fig.9, T_i^{CX} is 10 - 30 % lower than T_{i0}. This result is consistent with the above numerical analysis.

5. Neutral Density Measurement

Figure 10 shows the charge exchange spectra by the vertical NPA,

corresponding to different times of a divertor discharge. We can see that the charge exchange flux decreases with increasing $\bar{n}_e$. The dependence of the count rates of fast neutrals on $\bar{n}_e$ is shown in Fig.11. The rapid decrease in count rate is thought to be due to the decrease in neutral density in the plasma and due to the increase in plasma opacity for charge-exchanged neutrals. At $\bar{n}_e \lesssim 1.0\times10^{19} m^{-3}$, the count rates abruptly go down with decreasing $\bar{n}_e$. Most plausible explanation for this variation is that the ion temperature decreases with decreasing $\bar{n}_e$ owing to the reduction of equipartition between electrons and ions.

Generally, neutral density can be obtained by measuring the Hα or Dα radiation. The spectroscopic measurement, however, is not applicable for the determination of the neutral density in the core plasma, because the radiation signals are so weak and flat in intensity in the central plasma that Abel inversion has lots of uncertainties in the central neutral density determination. In order to estimate the birth profile and the attenuation rate of the flux, we used the 1-D neutral transport code. This code calculates neutral density profile by Monte Carlo method. The boundary condition, i.e. neutral density at the plasma boundary is given from Hα emission measurements.

Neutral density is estimated from charge exchange flux by the following expression,

$$n_0 = \frac{\sqrt{2\pi m T_i}\, N_D T_i}{4\sigma_{cx} n_i V_{eff} E \Delta E \eta_s \eta_D A} \frac{4\pi}{\Delta\Omega} e^{-E/T_i} \qquad (1)$$

where n_0 is the neutral density, n_i the ion density, $\Delta\Omega$ the observation solid angle, A the attenuation factor of the neutral flux, V_{eff} the effective observation volume mentioned below, m the mass of plasma ion, η_D the detector efficiency, and η_s and $\Delta E/E$ represent the stripping

efficiency and the energy resolution of the analyser. We measured the count rate, N_D, of the neutrals with E=15keV in order to obtain the neutral density in the core plasma, because these fast neutrals were generated near the core plasma under our experimental conditions. Since oxygen is a dominant impurity in experimental conditions described in the present paper, we estimated ion density (n_i) in eq.(1) from the experimental data of effective ion charge Z_{eff} by the equation, $n_i=(8-Z_{eff})\bar{n}_e/7$: Z_{eff} measured by spectroscopic measurements decreases with $\bar{n}_e$, and the value are 2.0 - 3.5 at $\bar{n}_e=1\times10^{19}m^{-3}$ and 1.7 - 2.6 at $\bar{n}_e=2\times10^{19}m^{-3}$.[10] Figure 12 shows the radial weight functions indicating the birth profiles of the neutrals with certain energies at $n_{i0}=n_{e0}=2\times10^{19}m^{-3}$, which were calculated by the neutral transport code. In this simulation, we assumed the density profile of $(1-(r/a)^2)^{0.3}$ and the temperature profile of $(1-(r/a)^2)$. Also we assumed $n_i(r)=n_e(r)$, T_{i0} =2.5 keV and T_{e0} = 3.0 keV. The observation volume, V_{eff}, and the attenuation factor, A, in eq.(1) were estimated from the radial birth profile. We can see from the figure that the fast neutrals are generated in somewhat wide region. Fortunately, such bad spatial resolution causes little error in the neutral density measurement, since the fast neutrals with 10 - 20 keV are generated in the region of $r/a<0.5$ where the expected neutral density is almost constant as shown in Fig.13.

Figure 14 shows the measured neutral density in the central region in the divertor discharges. These data were obtained from the charge exchange fluxes of the vertical NPA since the spectra of the NPA has little significant distortion in this configuration. We could not measure n_0 at $\bar{n}_e>4.5\times10^{19}m^{-3}$, because of the attenuation of the fast neutrals with 15 keV. As shown in the figure, n_0 decreases rapidly with increasing $\bar{n}_e$ at $\bar{n}_e\lesssim3\times10^{19}m^{-3}$. The reason is that the number of

Franck-Condon neutrals (~5eV) and their generations penetrating the core plasma decreases with $\bar{n}_e$ because of the ionization of the neutrals in the peripheral plasma. At $\bar{n}_e=3\times10^{19}m^{-3}$, n_0 is in the range of $(0.2\text{-}1)\times10^{11}m^{-3}$.

In large tokamaks such as JT-60 where $a\gg\lambda_{cx}$ is satisfied (where $\lambda_{cx}=\langle v\rangle/(n_i\langle\sigma v\rangle_{cx})$), a rough estimate of the neutral density can be made by treating the neutrals in the fluid approximation: in this case we can describe the neutral density by the following diffusion equation,[11]

$$\frac{\partial n_0}{\partial t}=\nabla D\nabla n_0-\frac{n_0}{\tau_{ii}}+S_0 \tag{2}$$

where D is the diffusion coefficient approximated by $\lambda_{cx}\langle v\rangle/3$, τ_{ii} is the ion-impact and electron-impact ionization time for the neutrals ($\tau_{ii}=\lambda_{ii}/\langle v\rangle$), and S_0 represents the source of neutrals. When the penetration of cold neutrals into the plasma is negligible compared with electron-ion recombination, the source term S_0 is given as follows,

$$S_0=n_i n_e\langle\sigma v\rangle_{rec} \tag{3}$$

where $\langle\sigma v\rangle_{rec}$ represents the rate coefficient for electron-ion recombination and can be approximated by,[12]

$$\langle\sigma v\rangle_{rec}\cong 1.27\times10^{-19}\frac{\zeta^{1.5}}{\zeta+0.59}\quad m^3/s \tag{4}$$

$$\zeta=13.6/T_e(eV)$$

Under our plasma parameters, the diffusion term ($\nabla D\nabla n_0$) is estimated to be negligibly small compared with the second and third terms on the right in eq.(2). Thus, substituting eq.(3) into eq.(2), the neutral

density n_0^{rec} by electron-ion recombination in steady state is obtained by the following expression,

$$n_0^{rec}=\frac{n_e n_i \langle\sigma v\rangle_{rec}}{n_e\langle\sigma v\rangle_{ei}+n_i\langle\sigma v\rangle_{ii}} \tag{5}$$

where $\langle\sigma v\rangle_{ei}$ is the rate coefficient for electron-impact ionization and $\langle\sigma v\rangle_{ii}$ is that for ion-impact ionization.

Open circles in Fig.14 represent the central neutral density determined from the count rate of neutrals with E=15keV, and solid lines show the neutral density expected from recombination alone, n_0^{rec}, at T_{e0}=2, 3 and 4keV. At $\bar{n}_e>3\times10^{19}m^{-3}$, the measured n_0 agrees with n_0^{rec} expected from recombination. This result indicates that the dominant process determing the central neutral density is electron-ion recombination at $\bar{n}_e\gtrsim2.5\times10^{19}m^{-3}$ and the density is independent of the influx of recycling or refuelling neutrals.

6. Discussion

In Sec.5, we concluded from the comparison of the experimental and the calculated neutral densities that the neutrals in the core plasma were principally produced by recombination at $\bar{n}_e\gtrsim2.5\times10^{19}m^{-3}$. In this section, we review the neutral density due to recombination.

The rate coefficient given by eq.(4), $\langle\sigma v\rangle_{rec}$, is expressed by T_e alone. To be accurate, however, $\langle\sigma v\rangle_{rec}$ depends on both T_e and the plasma density. The reasons suggesting the density-dependence are as follows: (i) neutral production rate due to three-body collision increases with plasma density; (ii) since excitation followed by ionization occurs often with increasing plasma density, the effective ionization rate of the

density n_0^{rec} by electron-ion recombination in steady state is obtained by the following expression,

$$n_0^{rec}=\frac{n_e n_i \langle\sigma v\rangle_{rec}}{n_e\langle\sigma v\rangle_{ei}+n_i\langle\sigma v\rangle_{ii}} \tag{5}$$

where $\langle\sigma v\rangle_{ei}$ is the rate coefficient for electron-impact ionization and $\langle\sigma v\rangle_{ii}$ is that for ion-impact ionization.

Open circles in Fig.14 represent the central neutral density determined from the count rate of neutrals with E=15keV, and solid lines show the neutral density expected from recombination alone, n_0^{rec}, at T_{e0}=2, 3 and 4keV. At $\bar{n}_e>3\times10^{19}m^{-3}$, the measured n_0 agrees with n_0^{rec} expected from recombination. This result indicates that the dominant process determing the central neutral density is electron-ion recombination at $\bar{n}_e\gtrsim2.5\times10^{19}m^{-3}$ and the density is independent of the influx of recycling or refuelling neutrals.

6. Discussion

In Sec.5, we concluded from the comparison of the experimental and the calculated neutral densities that the neutrals in the core plasma were principally produced by recombination at $\bar{n}_e\gtrsim2.5\times10^{19}m^{-3}$. In this section, we review the neutral density due to recombination.

The rate coefficient given by eq.(4), $\langle\sigma v\rangle_{rec}$, is expressed by T_e alone. To be accurate, however, $\langle\sigma v\rangle_{rec}$ depends on both T_e and the plasma density. The reasons suggesting the density-dependence are as follows: (i) neutral production rate due to three-body collision increases with plasma density; (ii) since excitation followed by ionization occurs often with increasing plasma density, the effective ionization rate of the

produced neutrals is affected by the density. Here, three-body collision means the following reaction,

$$e + e + H^{+} \text{ ---> } H(nl) + e$$

where nl stands for an energy level of a produced hydrogen atom. For an optically thick plasma, one must take account of reabsorption of photons which are emitted by the transition of excited hydrogen atoms. Thus, calculation including the influence of excited atoms must be performed to obtain the accurate density of neutrals produced by recombination.

Johnson and Hinnov[13] solved transition rate equations for atomic hydrogen and obtained coefficients for population of excited levels and for ionization and recombination. According to their calculation, the expected neutral density by recombination is given as follows,

$$n_o^{rec} = \frac{\alpha}{S} n_i + \frac{1}{n_e S}\left(\frac{dn_e}{dt} + \eta \frac{dn_o^{rec}}{dt}\right) \tag{6}$$

where α is the effective recombination coefficient, and S and η are coefficients determined by plasma density and temperature. From eq.(6), n_0^{rec} in steady state is given by $n_0^{rec}=n_i\alpha/S$. Figure 15 shows α and S calculated by them. This figure indicates that α and S are almost independent of n_e. The coefficients α and S at T_e=3keV in JT-60 are 1.1×10^{-22} m^3/s and 1.5×10^{-14} m^3/s, respectively: the central plasma of JT-60 is optically quite thin because $1/(\sigma_{abs}n_0) \gg \alpha$ is always satisfied (here, σ_{abs} stands for the Lyman-lines absorption cross section including exitation and ionization). Thus, we obtain $n_0^{rec}=7.3\times10^{-9}n_i$ m^{-3} . This agrees with the values from eq.(5). This result supports that neutrals in the central region are produced by recombination at $\bar{n}_e>2.5\times10^{19}m^{-3}$.

7. Conclusions

We measured the energy spectra of the charge-exchanged fast neutrals in ohmically heated JT-60 plasmas, using two NPAs with different sight-lines.

In the limiter discharges, we observed the enhancement of low-energy charge exchange fluxes by the NPA viewing near the limiter plate. In the divertor configuration, the enhancement was observed by the divertor-side NPA. These results indicate that there is the striking poloidal asymmetry of neutral sources near the plasma boundary and that this asymmetry influences on the neutral density profile in the plasma.

The measured ion temperature from charge exchange was 10-30% lower than T_{i0} at $\bar{n}_e=(0.5\text{-}4.0)\times10^{19}m^{-3}$. Numerical analysis using the neutral transport code supports this result. The numerical results also indicate that T_i^{CX}/T_{i0} does not depend on the plasma temperature nor the density profiles but the plasma density.

Neutral density from charge exchange measurements decreased with $\bar{n}_e$ at $\bar{n}_e\lesssim3\times10^{19}m^{-3}$, owing to rapid decrease of Franck-Condon neutrals and their generations penetrating the core plasma. At $\bar{n}_e=3\times10^{19}m^{-3}$, n_0 was in the range of $(0.2\text{-}1)\times10^{11}m^{-3}$. For the plasma with $\bar{n}_e\gtrsim2.5\times10^{19}m^{-3}$, the measured n_0 was in agreement with the neutral density expected from electron-ion recombination alone. The result indicates that the neutrals in the core plasma are principally generated by electron-ion recombination at $\bar{n}_e\gtrsim2.5\times10^{19}m^{-3}$.

Acknowledgements

The authors would like to thank Dr. N. Nishino for useful discussion on atomic processes, and Dr. A. Funahashi for his valuable comment and encouragement. We also wish to acknowledge Drs. Y. Suzuki, S. Tamura and M. Yoshikawa for their continuing encouragement throughout this work.

References

1) Gaudreau, M. P. J., Kyslyakov, A. I., Sokolov, Yu. A., Nucl. Fusion 18(1978)1725.

2) Dnestrovskij, Yu. N., Lysenko, S. E., Kyslyakov, A. I., Nucl. Fusion 19(1979)239.

3) JT-60 Team, Plasma Phys. 28(1986)165.

4) Nemoto, M., et al., to be published

5) Hayashi, K., Hashimoto, K., Yamato, H., Takeuchi, H., et al., Rev.Sci.Instrum. 56(1985)359.

6) Gott, Yu. V., Yurchenko, E. I., Sov. J. Plasma Phys. 9(1983)377.

7) Yamada, K., Koide, Y., Shimizu, K., Hirayama, T., et al., Japan Atomic Energy Research Institute Rep. JAERI-M Rep. JAERI-M 86-057 (1986).

8) Tsuji, S., Hayashi, K., Yoshida, H., Hosogane, N., et al., ibid. JAERI-M 86-006(1986) (in Japanese).

9) Tobita, K., Kusama, Y., Nemoto, M., Takeuchi, H., et al., Bul. Amer. Phys. Soc. 32(1987)1768.

10) JT-60 Team, in Plasma Physics and Controlled Nuclear Fusion Research (Proc. 11th Int. Conf. Kyoto, 1986), Vol.1 IAEA, Vienna (1986)11.

11) Goldston, R. J., Princeton Plasma Physics Laboratory Rep. PPPL-1924(1982).

12) Gordeev, Yu. S., Zinov'ev, A. I., Petrov, M. P., JETP. Letters 25(1977)204.

13) Johnson, L. C., Hinnov, E., J. Quant. Spectrosc. Radiat. Transfer 13(1973)333.

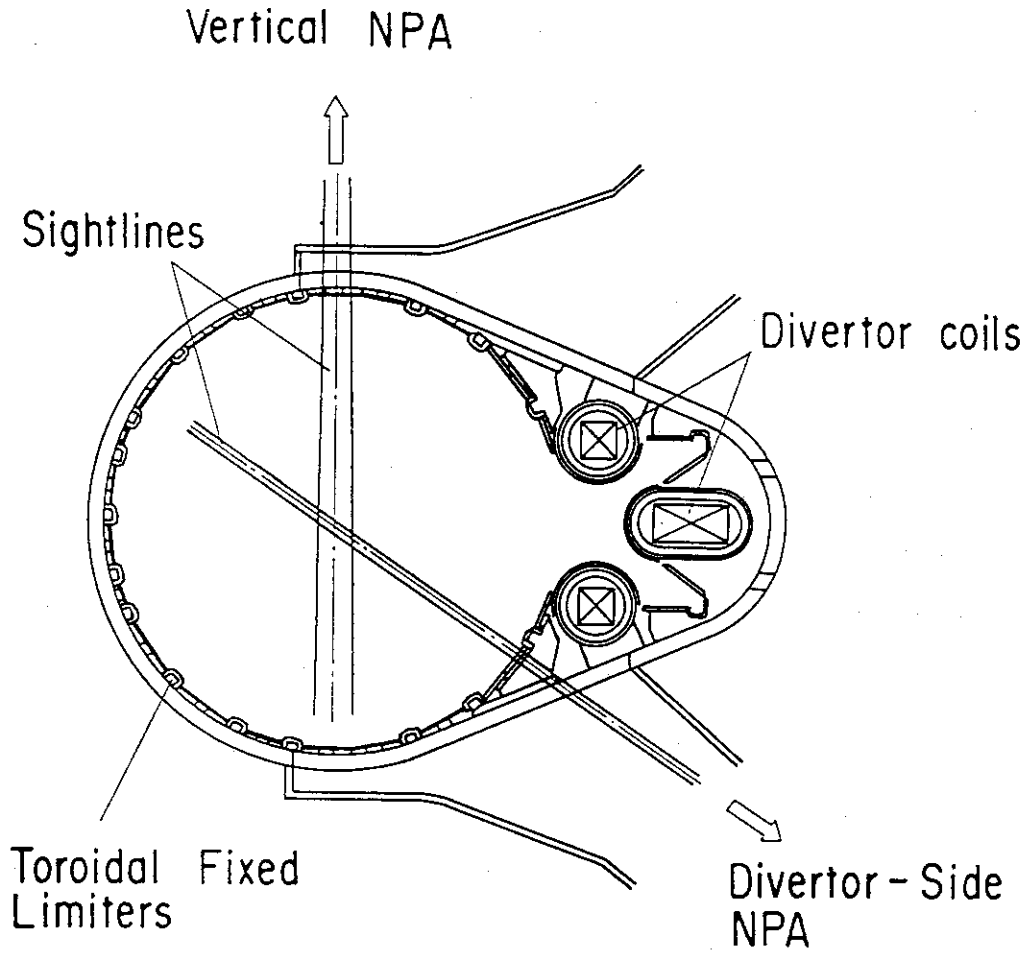

Fig.1 Poloidal cross section of JT-60 and sight-lines of the neutral particle analysers (NPA).

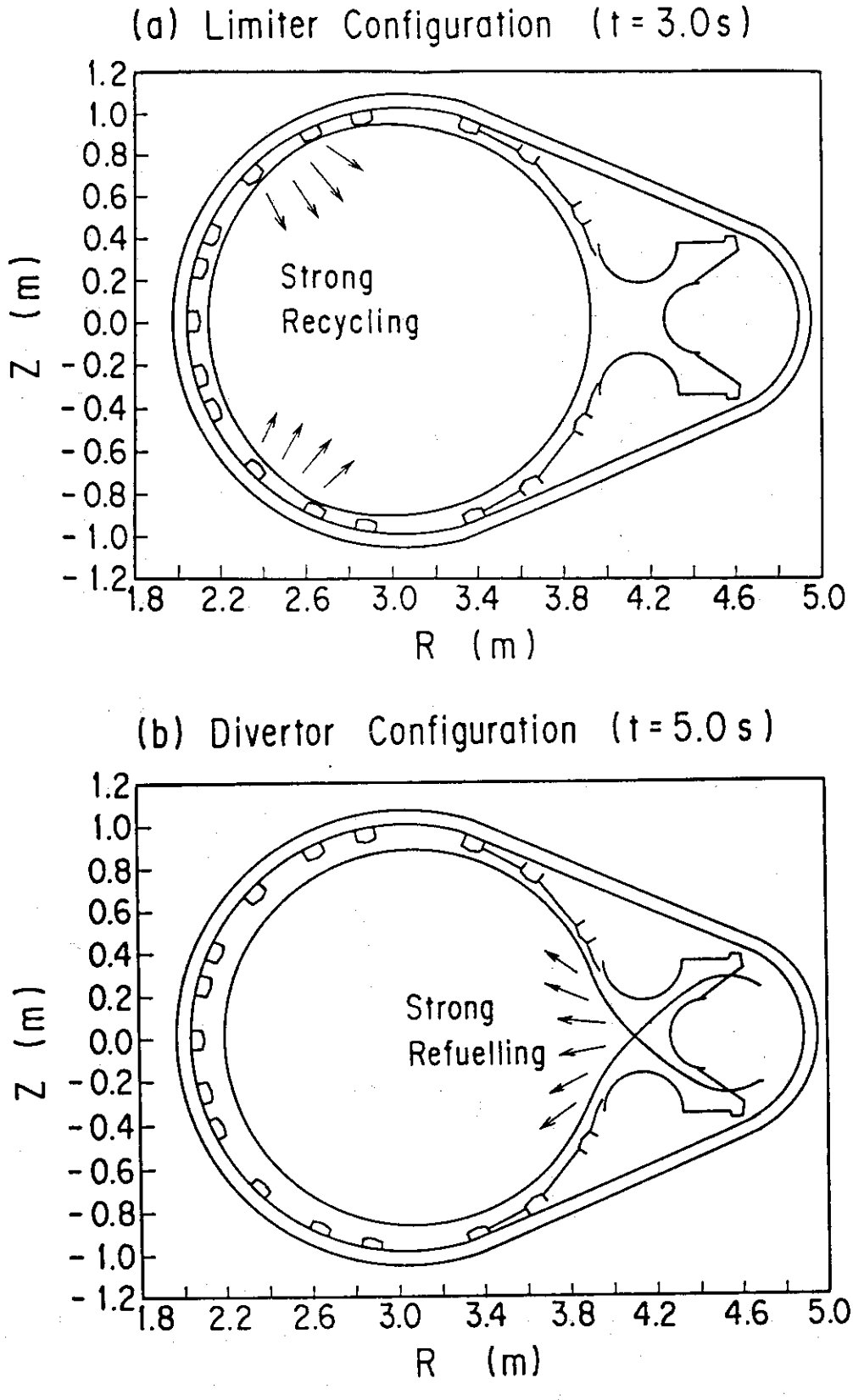

Fig.2 Most outer magnetic surfaces of the limiter and divertor configuration of JT-60 plasmas. Arrows represent the expected flows of cold neutrals.

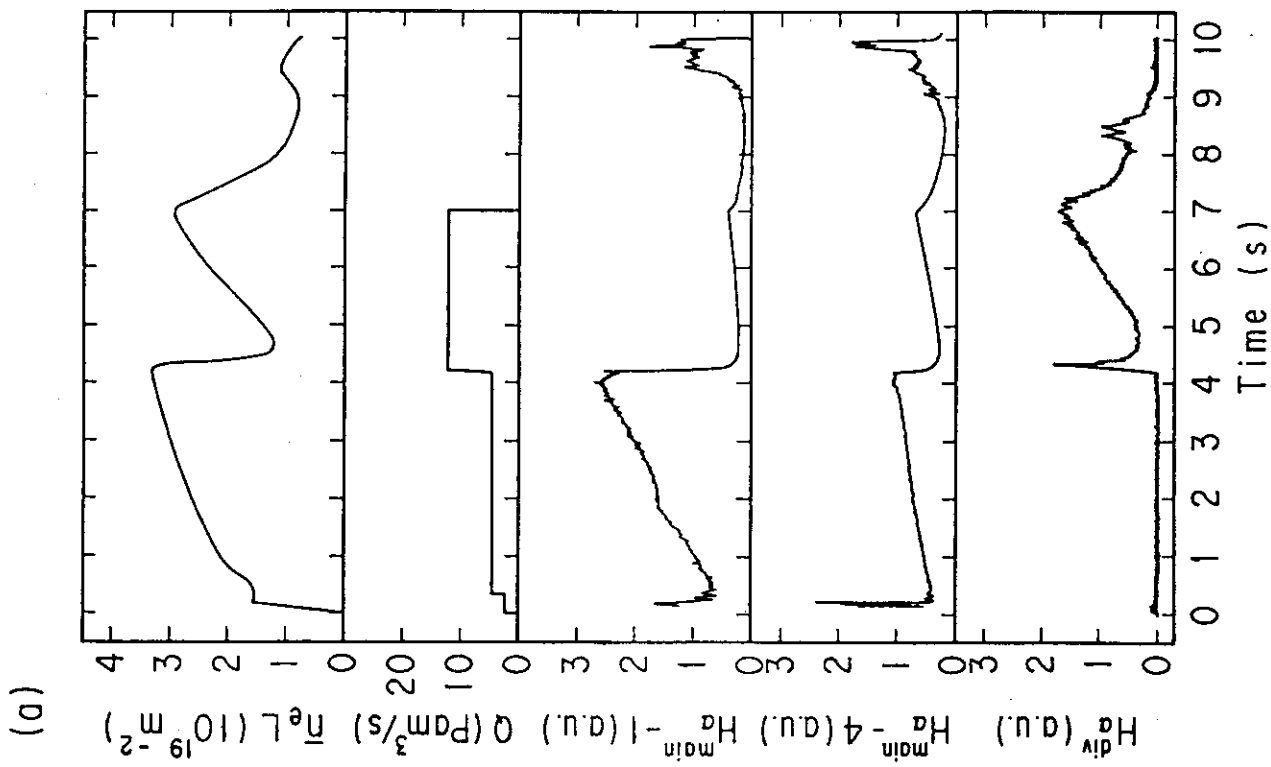

Fig.3 Time evolution of $\bar{n}_e L$, Q, and Hα emissivities, and sight-lines of photo-diodes for Hα emission measurements.

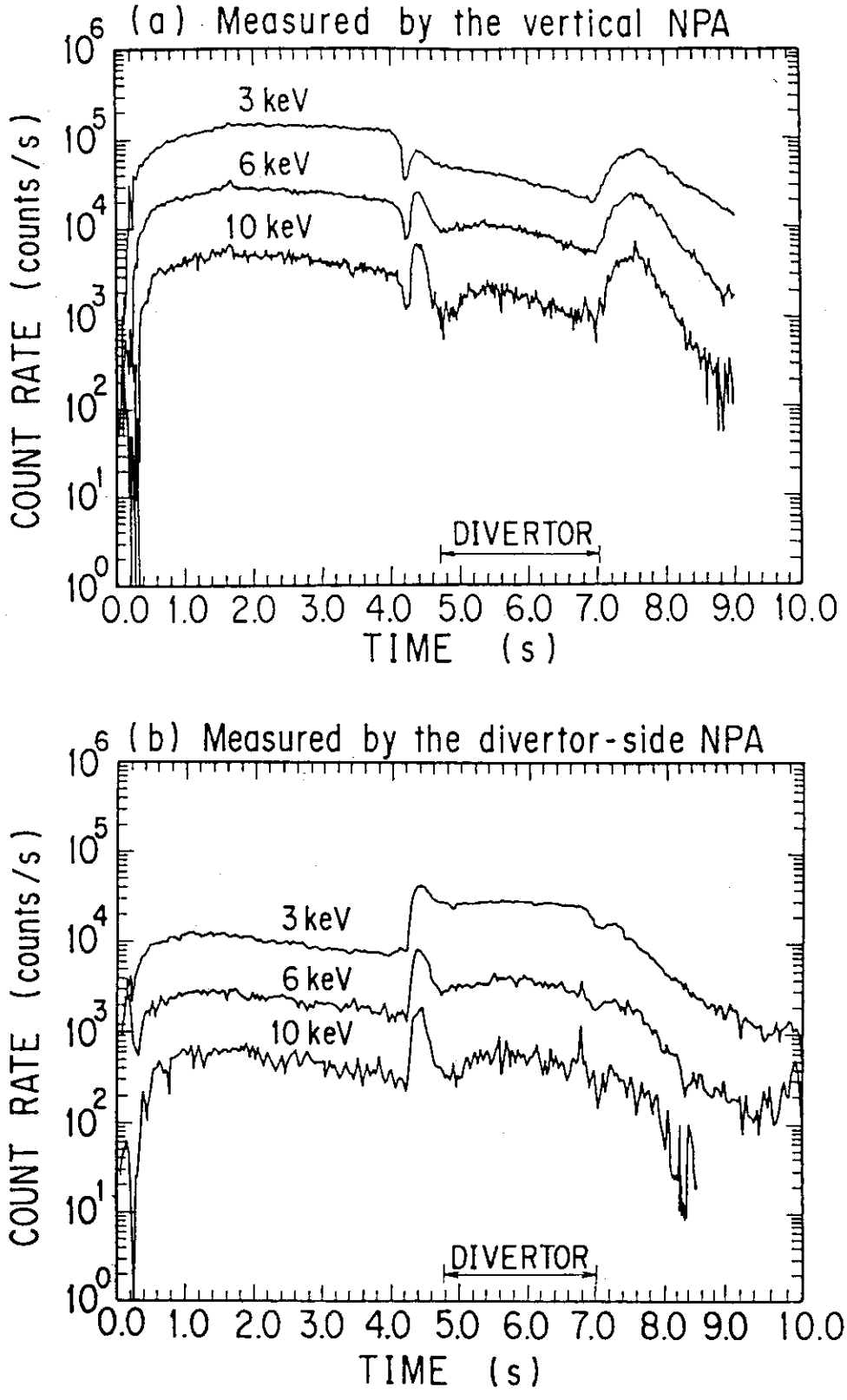

Fig.4 Time evolution of charge exchange fluxes.
Solid lines represent the fluxes for the charge-exchanged with the energy of 3, 6 and 10 keV.
(a) The fluxes measured by the vertical NPA.
(b) The fluxes measured by the divertor-side NPA.

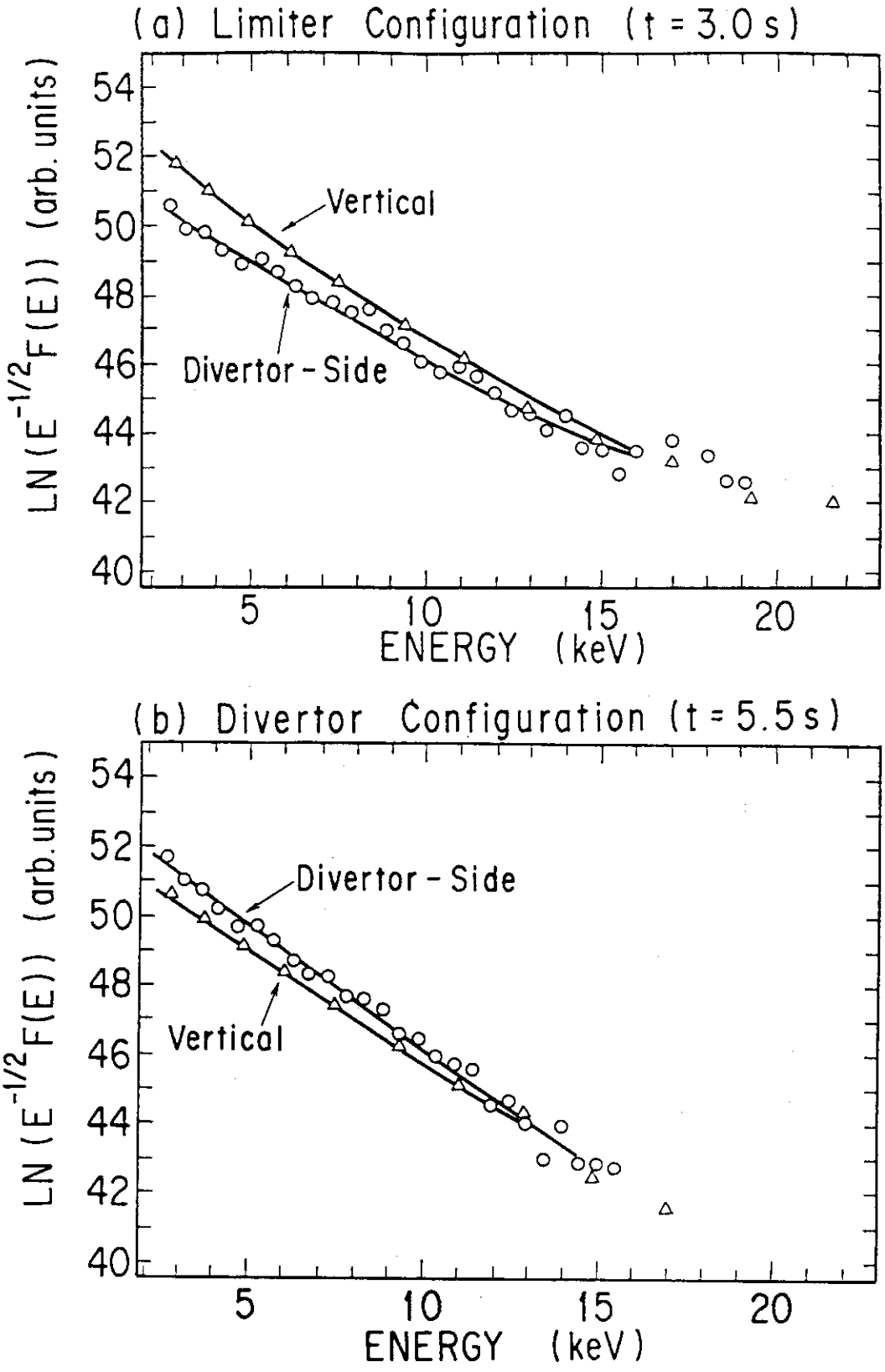

Fig.5 Distortion of charge exchange spectra due to poloidal asymmetry of neutral sources. (a) The spectra obtained in the limiter configuration (t=3.0s).(b) The spectra obtained in the divertor configuration (t=5.5s). The spectra are compared in same observation volume and solid angle.

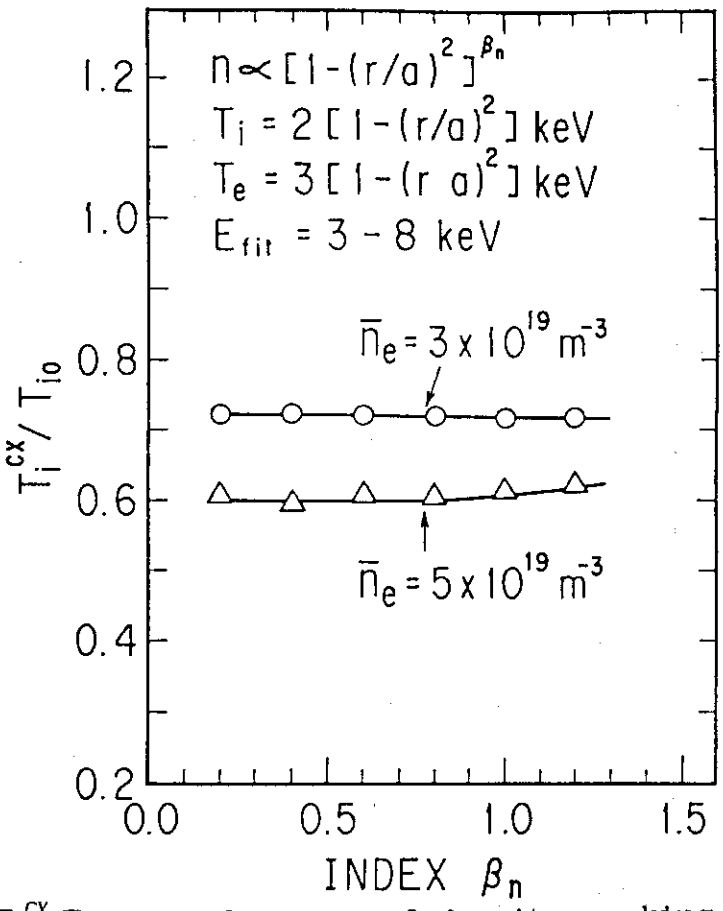

Fig.6 T_i^{CX}/T_{i0} as a function of density peaking factor.

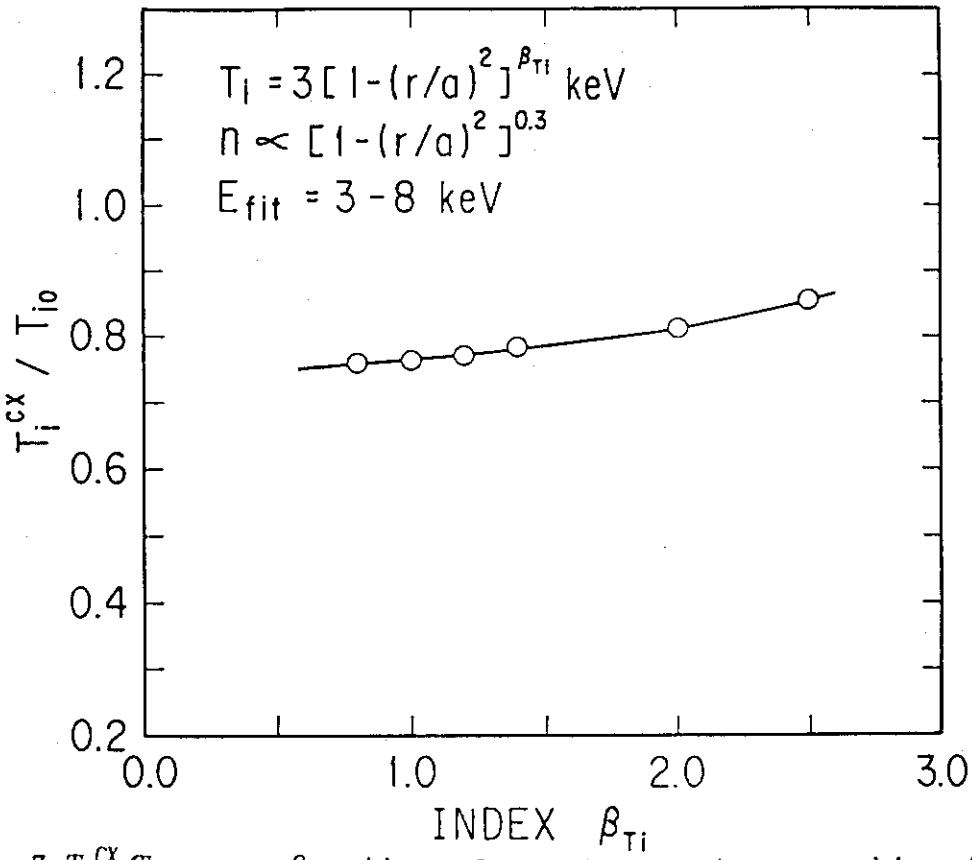

Fig.7 T_i^{CX}/T_{i0} as a function of ion temperature peaking factor.

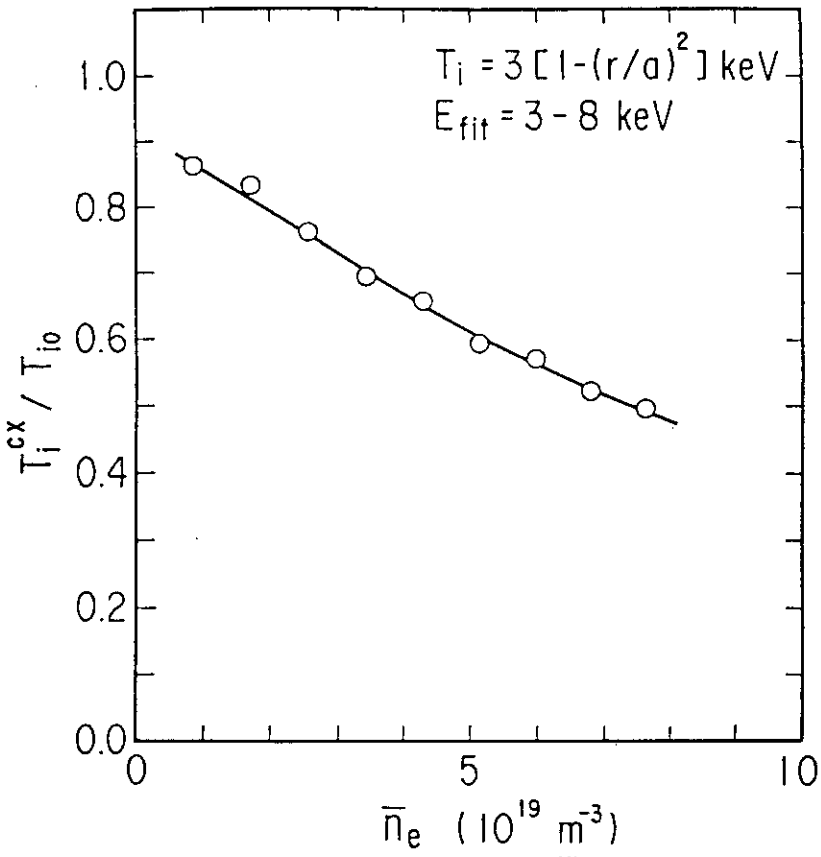

Fig.8 Dependence of T_i^{CX}/T_{i0} on $\bar{n}_e$.

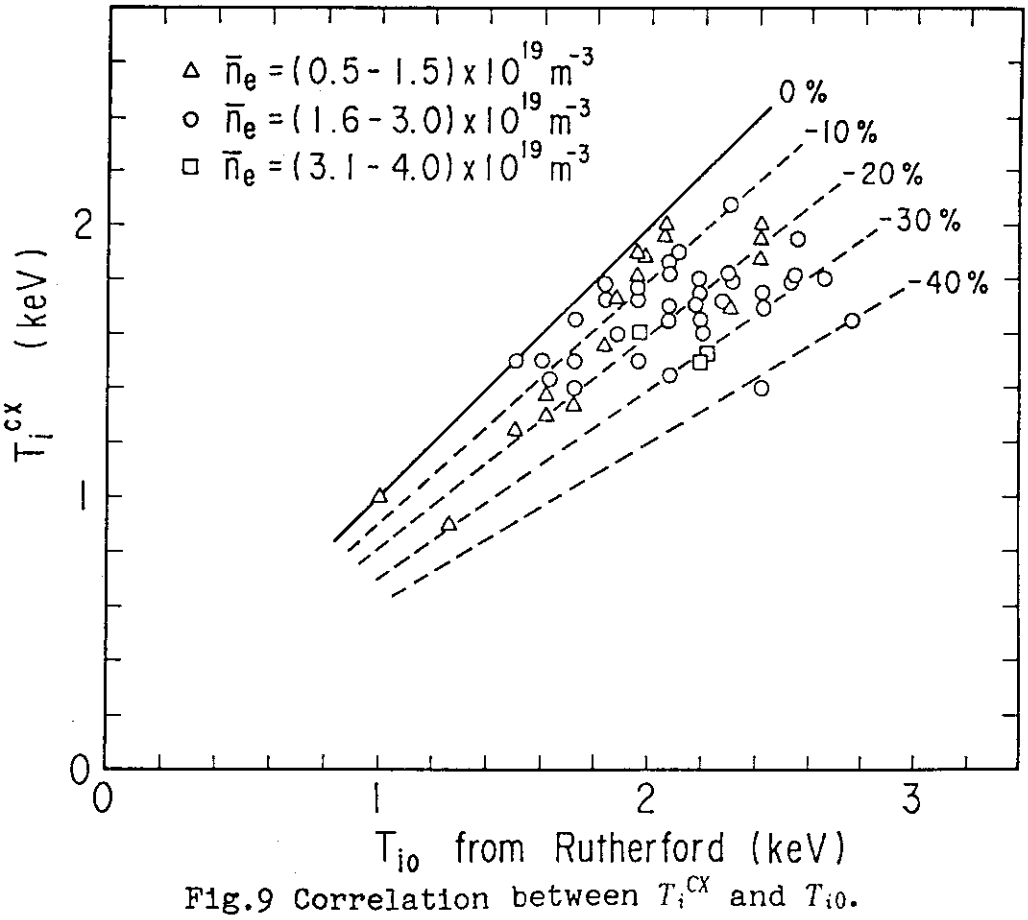

Fig.9 Correlation between T_i^{CX} and T_{i0}.

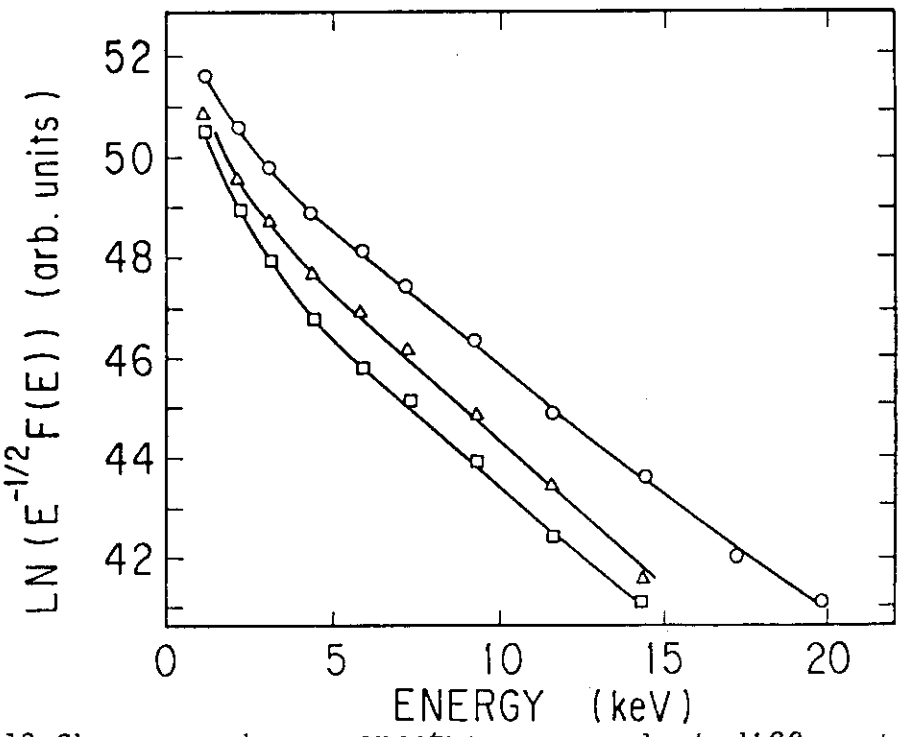

Fig.10 Charge exchange spectra measured at different times.
○ - 2.0s, $\bar{n}_e$=1.1×10^{19}m^{-3}
△ - 3.0s, $\bar{n}_e$=1.9×10^{19}m^{-3}
□ - 4.0s, $\bar{n}_e$=2.6×10^{19}m^{-3}

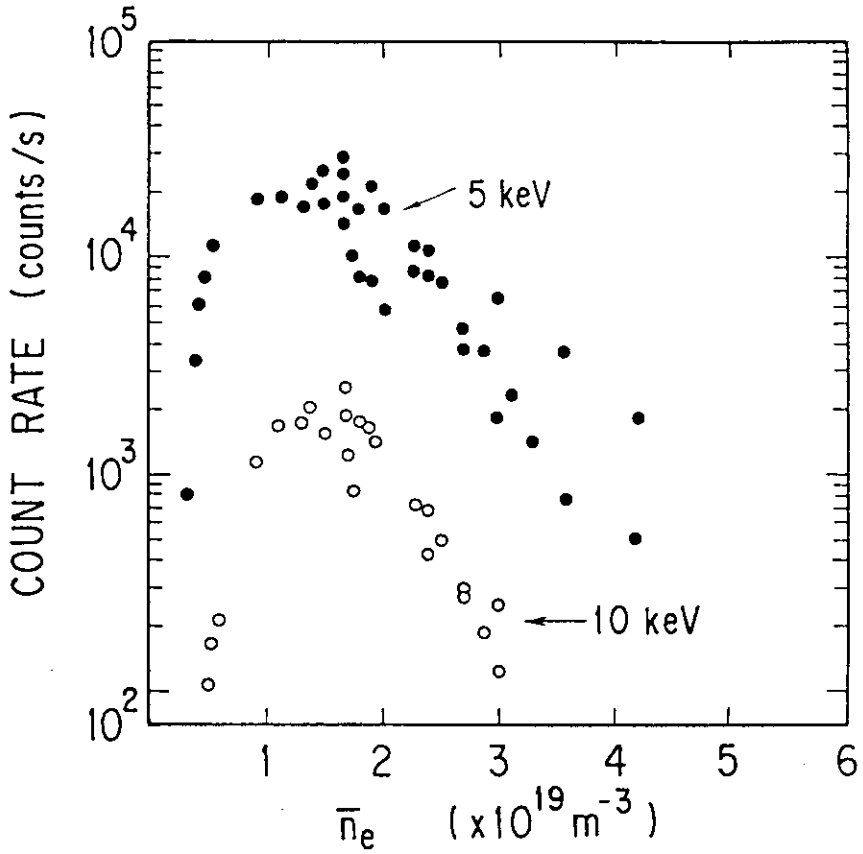

Fig.11 Count rates of fast neutrals with 5 keV and 10 keV, as a function of line-averaged electron density.

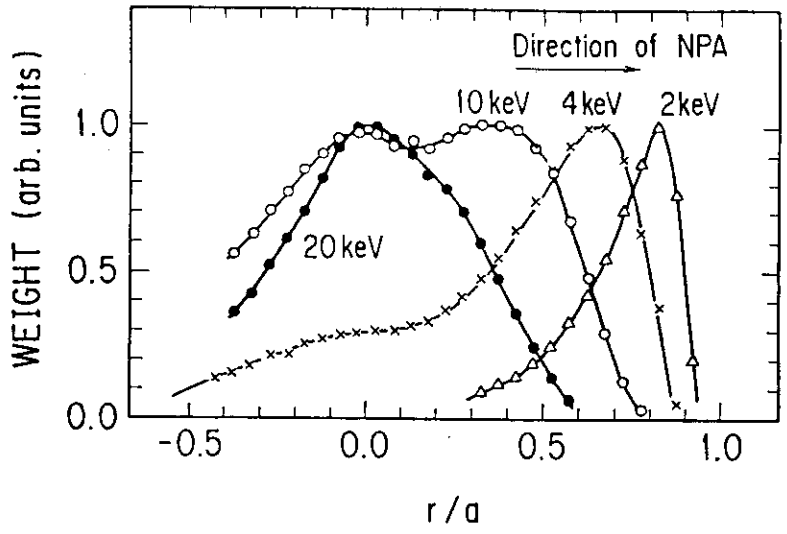

Fig.12 Numerical result showing the birth profiles of fast neutrals contributing charge exchange spectra under the condition of $n_{e0}=n_{i0}=2\times10^{19}m^{-3}$, $T_{e0}=3.0keV$ and $T_i=2.5keV$.

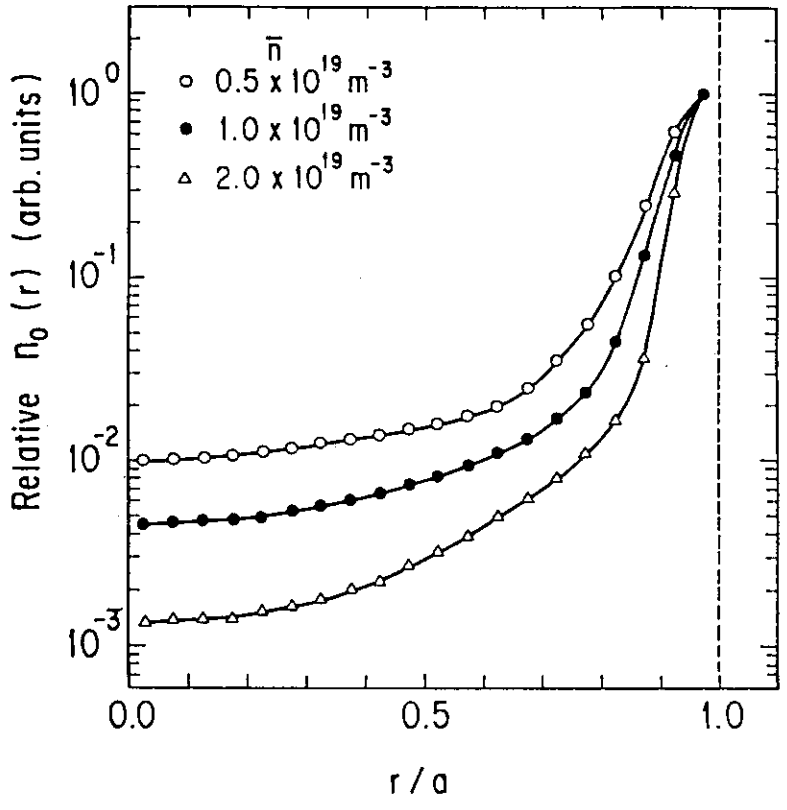

Fig.13 Relative neutral density profile calculated by the 1-D neutral transport code, under the condition of $n_{e0}=n_{i0}=2\times10^{19}m^{-3}$, $T_{e0}=3.0keV$ and $T_{i0}=2.5keV$.

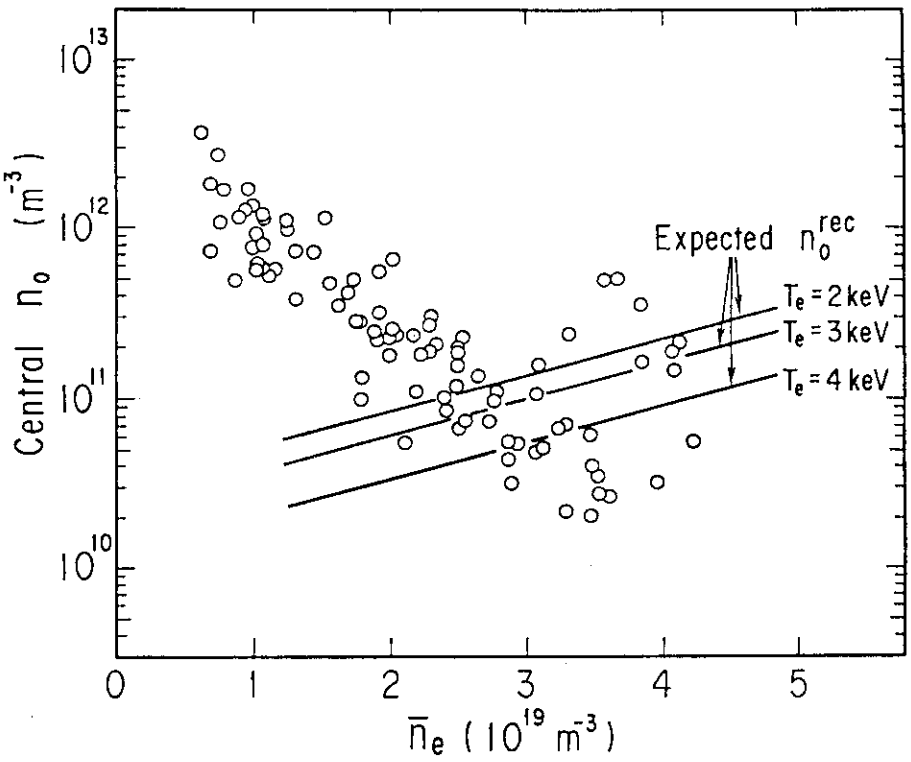

Fig.14 Measured neutral density near the plasma core as a function of $\bar{n}_e$.

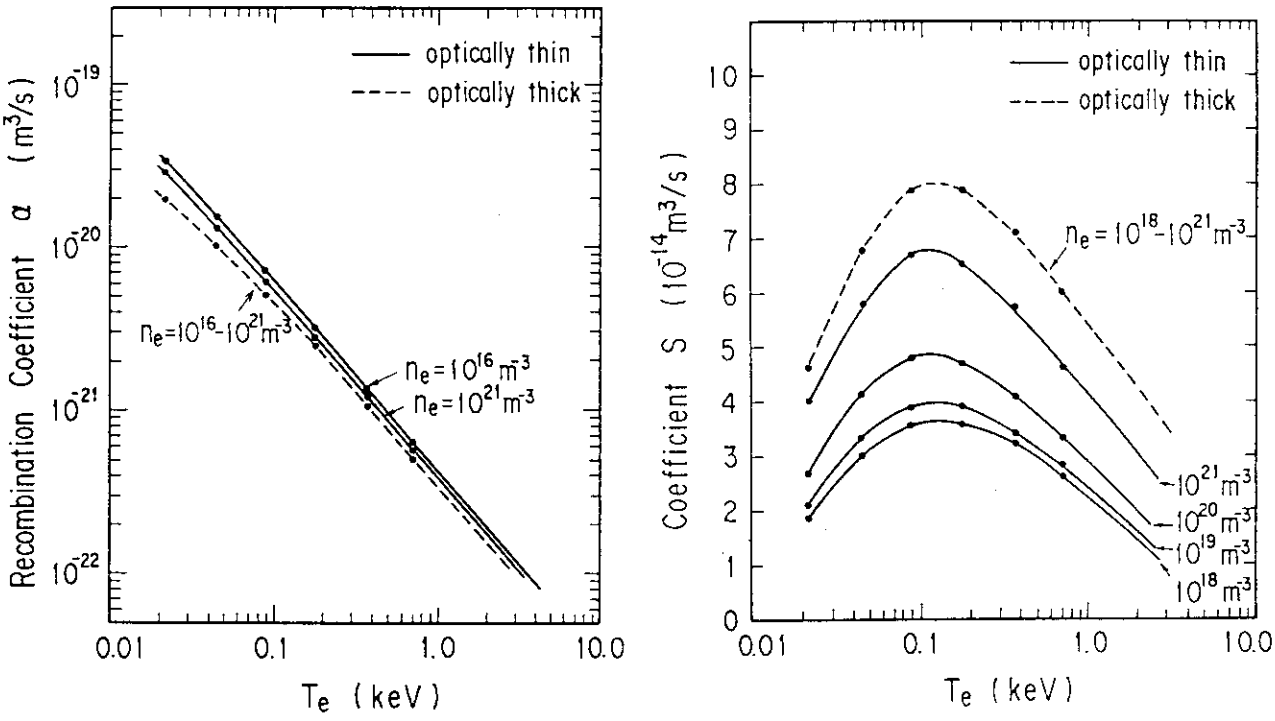

Fig.15 Coefficients α and S as a function of T_e.
Dots represent the calculated values by Johnson and Hinnov.[13]